

Supplementary Materials

Biomass-derived sustainable electrode material for low-grade heat harvesting

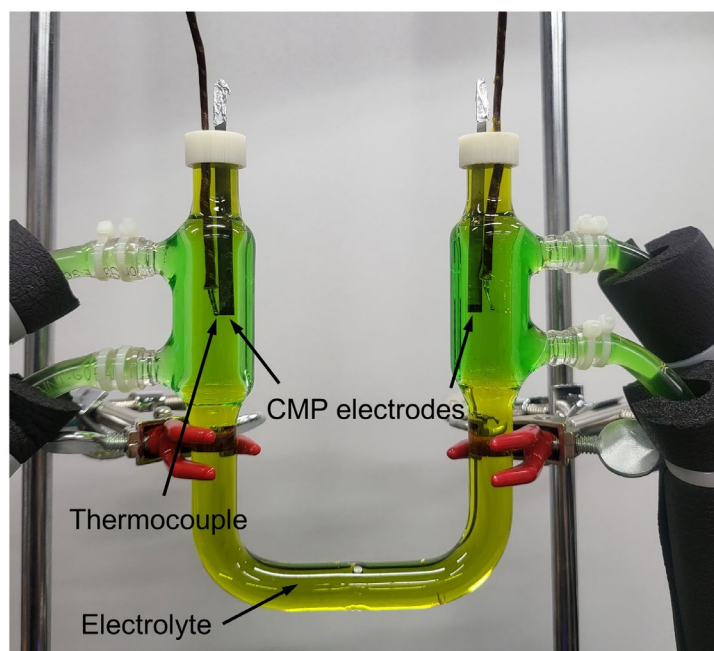


Figure S1. Experimental setup for measuring the temperature coefficient of the redox potential of $\text{Fe}(\text{CN})_6^{3-}/\text{Fe}(\text{CN})_6^{4-}$. Thermocouples were passivated with epoxy resin, preventing them from directly exposing the electrolyte.

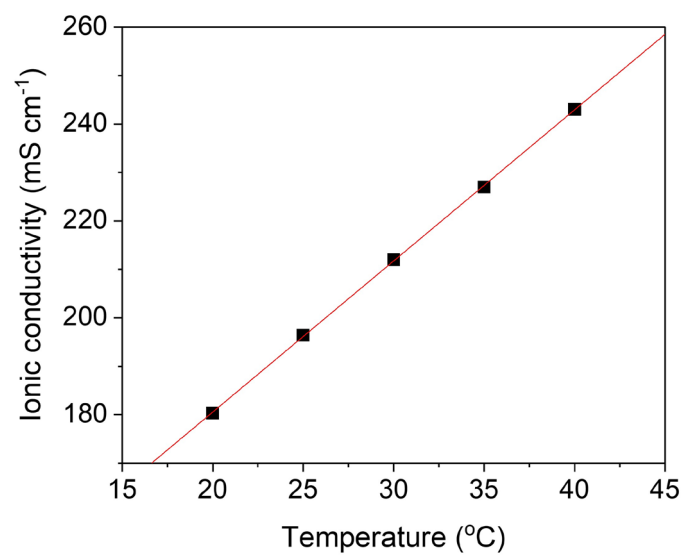


Figure S2. Dependence of ionic conductivity of 0.4 M $\text{Fe}(\text{CN})_6^{3-}/\text{Fe}(\text{CN})_6^{4-}$ electrolyte on temperature.

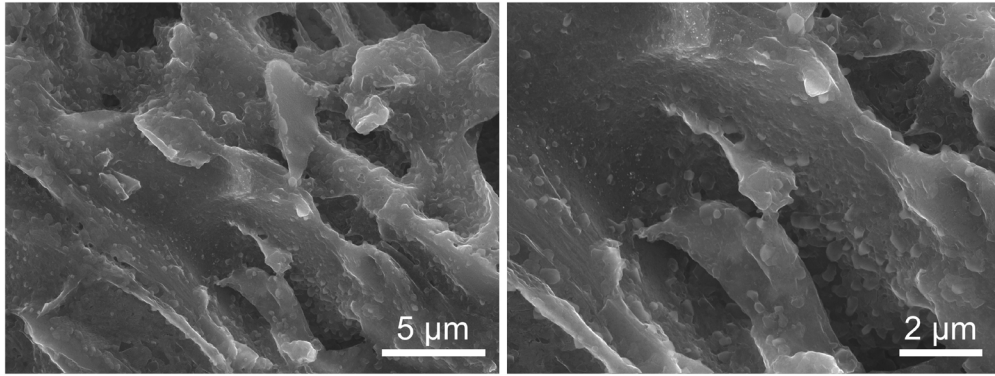


Figure S3. FESEM images of as-synthesized CMP-800 before washing with HCl and DI water.

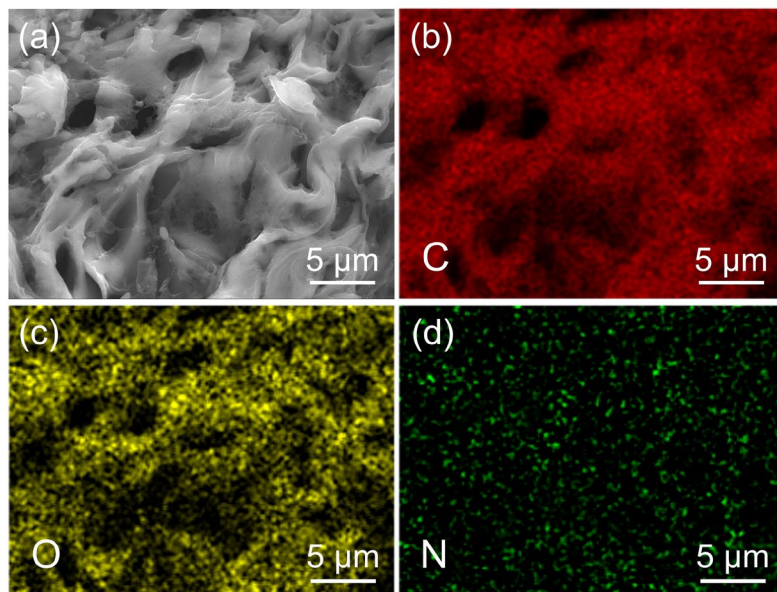


Figure S4. (a) FESEM and (b-d) EDS mapping images of AMP-800-1.

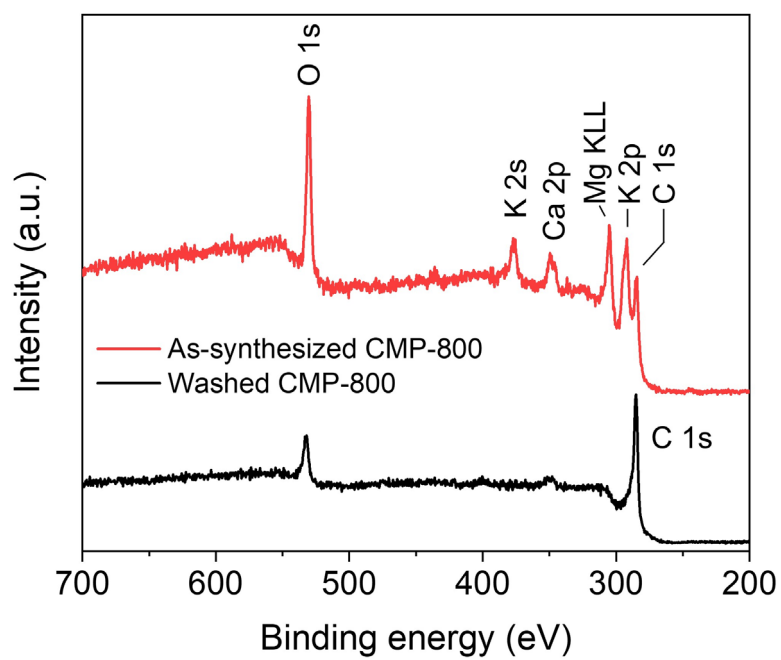


Figure S5. XPS survey spectra of as-synthesized CMP-800 and washed CMP-800.

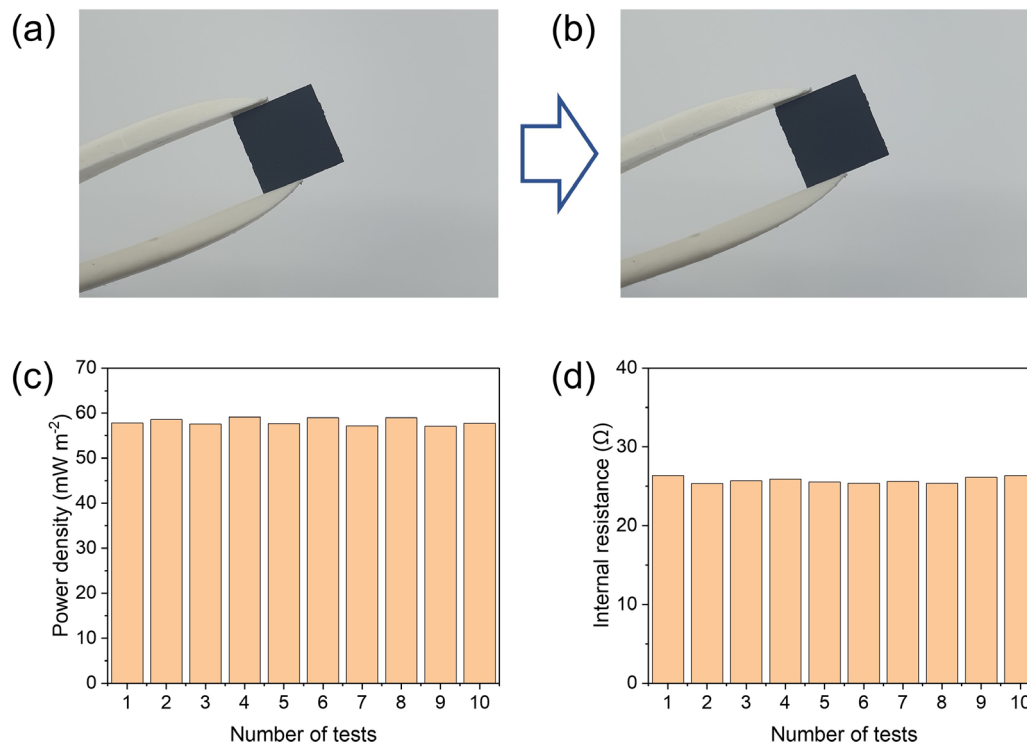


Figure S6. Optical images of a CMP-800 electrode (a) before and (b) after ten assembly and disassembly tests, (c) power density, and (d) internal resistance of thermocell with CMP-800 electrodes according to the number of tests.

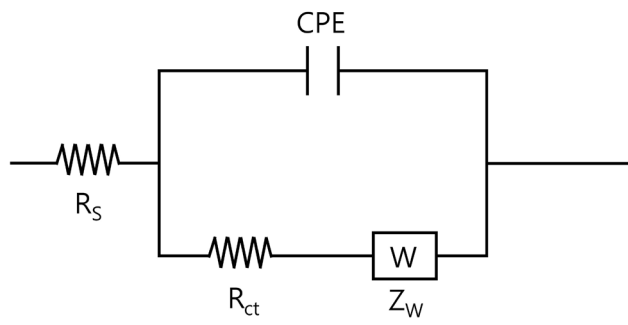


Figure S7. Equivalent circuit model of a thermocell for the analysis of EIS. R_s denotes the ohmic resistance, R_{ct} is the charge transfer resistance, Z_w accounts for the Warburg impedance, and CPE is the capacitance.

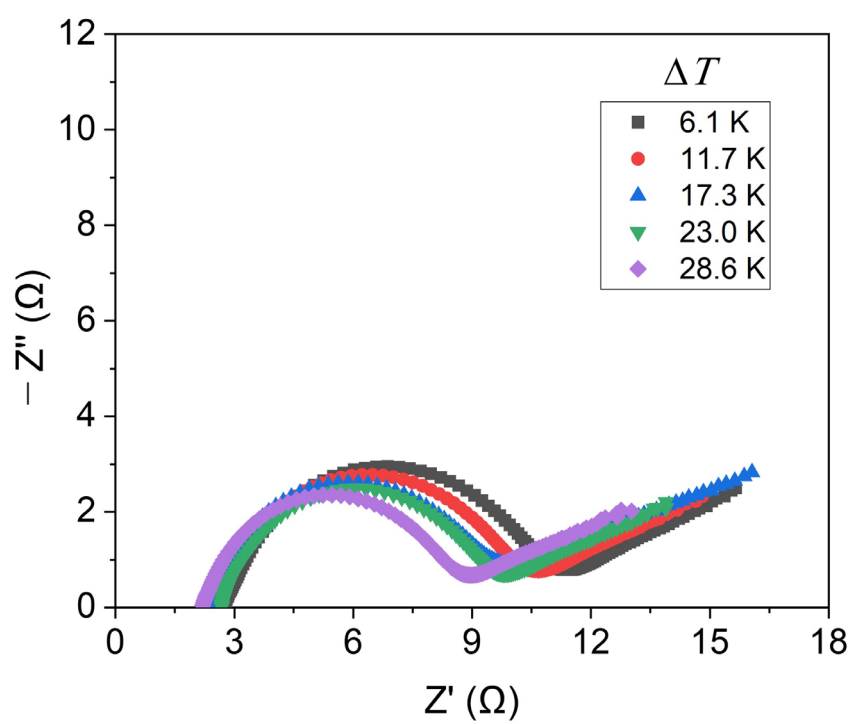


Figure S8. Nyquist plots of CMP-800 according to ΔT .